

Approximate Coulomb Distortion Effects in $(e, e'p)$ Reactions.

K.S. Kim and L.E. Wright

*Institute of Nuclear and Particle Physics, Department of Physics and Astronomy, Ohio
University, Athens, Ohio 45701*

Abstract

In this paper we apply a well-tested approximation of electron Coulomb distortion effects to the exclusive reaction $(e, e'p)$ in the quasielastic region. We compare the approximate treatment of Coulomb distortion effects to the exact Distorted Wave Born Approximation evaluated by means of partial wave analysis to gauge the quality of our approximate treatment. We show that the approximate Møller potential has a plane-wave-like structure and hence permits the separation of the cross section into five terms which depend on bi-linear products of transforms of the transition four current elements. These transforms reduce to Fourier transforms when Coulomb distortion is not present, but become modified with the inclusion of Coulomb distortion. We investigate the application of the approximate formalism to a model of $^{208}\text{Pb}(e, e'p)$ using Dirac-Hartree single particle wavefunctions for the ground state and relativistic optical model wavefunctions for the continuum proton. We show that it is still possible to extract, albeit with some approximation, the various structure functions from the experimentally measured data even for heavy nuclei.

25.30.Fj 25.70.Bc.

Typeset using REVTeX

I. INTRODUCTION

Medium and high energy electron scattering has long been acknowledged as a useful tool in the investigation of nuclear structure and nuclear properties, especially in the quasielastic region. In the plane wave Born approximation (PWBA), where electrons are described by Dirac plane waves, the cross section for the exclusive reaction $(e, e'p)$ on nuclei can be written simply as

$$\begin{aligned} \frac{d^3\sigma}{dE_f d\Omega_f d\Omega_P} &= \frac{PE_P}{(2\pi)^3} \sigma_M [v_L R_L + v_T R_T + \cos 2\phi_P v_{TT} R_{TT} \\ &\quad + \cos \phi_P v_{LT} R_{LT} + h \sin \phi_P v_{LT'} R_{LT'}] \end{aligned} \quad (1)$$

where $q_\mu^2 = \omega^2 - q^2$ is the four-momentum transfer, σ_M is the Mott cross section given by $\sigma_M = \left(\frac{\alpha}{2E}\right)^2 \frac{\cos^2 \frac{\theta}{2}}{\sin^4 \frac{\theta}{2}}$, and R_L , R_T , R_{TT} , R_{LT} , and $R_{LT'}$ are the longitudinal, transverse, transverse-transverse, longitudinal-transverse, and polarized longitudinal-transverse structure functions which depend only on the momentum transfer q and the energy transfer ω . The functions v only depend on electron kinematics and are given by

$$\begin{aligned} v_L &= \frac{q_\mu^4}{q^4} \\ v_T &= \tan^2 \frac{\theta_e}{2} - \frac{q_\mu^2}{2q^2} \\ v_{TT} &= -\frac{q_\mu^2}{2q^2} \\ v_{LT} &= -\frac{q_\mu^2}{q^2} \left(\tan^2 \frac{\theta_e}{2} - \frac{q_\mu^2}{q^2} \right)^{1/2} \\ v_{LT'} &= -\frac{q_\mu^2}{q^2} \tan \frac{\theta_e}{2} \end{aligned} \quad (2)$$

Choosing the momentum transfer \mathbf{q} to define the $\hat{\mathbf{z}}$ axis and using the azimuthal symmetry of the spatial part of the Møller potential permits the extraction of the explicit dependence on the azimuthal angle ϕ_P of the outgoing proton as measured with respect to the electron scattering plane. More specifically, we define $\hat{\mathbf{y}} = \hat{\mathbf{p}}_i \times \hat{\mathbf{p}}_f$. These structure functions are defined as:

$$\begin{aligned}
R_L &= \frac{q^4}{q_\mu^4} W_{00} \\
R_T &= W_{11} + W_{22} \\
\cos 2\phi_P R_{TT} &= W_{11} - W_{22} \\
\cos \phi_P R_{LT} &= -\frac{q^2}{q_\mu^2} (W_{01} + W_{10}) \\
\sin \phi_P R_{LT'} &= -i \frac{q^2}{q_\mu^2} (W_{02} + W_{20})
\end{aligned} \tag{3}$$

where the nuclear tensors $W_{\mu\nu}$ are given in terms of a sum over s_p and μ_p the final and initial spin projections of the nucleon,

$$W_{\mu\nu} = \sum_{s_p \mu_b} N_\mu^* N_\nu. \tag{4}$$

and we have suppressed the spin labels for clarity. The quantities N^μ are the Fourier transform of the nucleon current density $\mathbf{J}^\mu(\mathbf{r})$ given by

$$N^\mu = \int J^\mu e^{i\mathbf{q}\cdot\mathbf{r}} d^3r. \tag{5}$$

Current conservation and gauge invariance can be used to eliminate the z -components so that only N_0 , N_x , and N_y need to be calculated.

By keeping the momentum and energy transfer fixed while varying the electron energy E and scattering angle θ_e , or varying the azimuthal angle of the outgoing proton and the helicity of the incident electron, it is possible to extract from experiment the five structure functions as a function of momentum and energy transfer. However, when the electron wavefunctions are not Dirac plane waves, but rather are distorted by the static Coulomb field of the target nucleus, such a simple formulation as given in Eq. (1) is no longer possible. In the full Distorted Wave Born Approximation (DWBA) calculation, it is not possible to express the cross section as a sum of bi-linear products of transforms of transition current matrix elements which only depend on the electron kinematics and the outgoing proton's azimuthal angle. The key point is that the momentum transfer does not enter the analysis in a natural way. Of course, one could pretend that the plane-wave result is still valid and

extract the various "structure functions". However, there is no way in the DWBA approach to investigate these terms separately.

Using partial wave analysis, the Ohio University group [1]– [4] has treated the Coulomb distortion arising from the static Coulomb field of the nucleus exactly. Coupling the distorted waves with the one hard photon exchange approximation (Distorted Wave Born Approximation-DWBA) has allowed this analysis to be compared to data from a range of nuclei. The nuclear model used includes the following ingredients: 1) Relativistic Hartree single particle wavefunctions for the bound orbitals [5,6], 2) Relativistic optical model for the continuum proton [7], and 3) the free relativistic current operator for the proton with the standard form factors. This simple relativistic "one-body" model along with the exact treatment of Coulomb distortion is in excellent agreement with all the data involving knock-out from surface orbitals of nuclei that have been analysed. This includes nuclei as light as ^{16}O and as heavy as ^{208}Pb . However, for cases where the outgoing particle is in the continuum where all multipoles can contribute, the DWBA analysis requires extensive computer codes which require more and more time and precision as the energy increases. Furthermore, as noted above in the exact DWBA analysis, the cross section cannot be written as the sum of five terms which are bi-linear products of transforms of the transition current matrix elements. There two reasons have led researchers to seek an approximate treatment of Coulomb distortion that would permit the extraction of "structure" functions from experiment under conditions where the effects of Coulomb distortion in the different terms can be investigated, and could be easily extended to higher energies such as will be available at the Thomas Jefferson National Accelerator Facility.

In a previous paper [8] we investigated a rather extreme approximation of Coulomb distortion effects for the inclusive reaction (e, e') in the quasielastic region and using some *ad hoc* assumptions obtained excellent agreement with the exact DWBA calculations. In this paper, we apply a more exact approximation to the exclusive reaction $(e, e'p)$ and investigate its validity. One of our advantages as compared to previous investigators is that we have the full DWBA calculation to use as a standard in assessing the accuracy of our

approximation. In Section II we will give the approximate electron wavefunctions for the incoming and outgoing electron waves and derive the approximate Møller potential from these wavefunctions. In Section III we use the approximate Møller potential to calculate the differential cross section for $(e, e'p)$ and define the approximate Coulomb deformed structure functions. In Section IV we compare approximate and DWBA $(e, e'p)$ cross sections for so-called parallel and perpendicular kinematics and investigate the extraction from the cross sections of the so-called fourth (R_{LT}) and fifth ($R_{LT'}$) structure functions. In Section V we give our conclusions and discuss prospects for the future.

II. APPROXIMATE WAVEFUNCTIONS AND THE MÖLLER POTENTIALS

Following the work of Lenz and Rosenfelder [10], we propose the following plane-wave-like electron wavefunction [8,9] which contains the effects of the static Coulomb distortion of the target nucleus in an approximate way:

$$\Psi^{(\pm)}(\mathbf{r}) = \frac{p'(r)}{p} e^{\pm i\delta(\mathbf{J}^2)} e^{i\Delta} e^{i\mathbf{p}'(r)\cdot\mathbf{r}} u_p. \quad (6)$$

The (\pm) sign denotes incoming and outgoing boundary conditions for electrons of momentum \mathbf{p} , the phase factor $\delta(\mathbf{J}^2)$ is a function of the square of the angular momentum operator \mathbf{J} , and the local effective momentum $\mathbf{p}'(r)$ is given in terms of the Coulomb potential of the target nucleus by

$$\mathbf{p}'(r) = \left(p - \frac{1}{r} \int_0^r V(r) dr \right) \hat{\mathbf{p}}. \quad (7)$$

We refer to this r -dependent momentum as the Local Effective Momentum Approximation(LEMA). Some small higher order corrections have been incorporated into the *ad-hoc* term $\Delta = a(\hat{p}'(r)\cdot\hat{r})(\mathbf{J}^2 + \frac{1}{4})$ which involves the factor a which is parametrized by $a = -\alpha Z(\frac{16}{p})^2$ where Z is the charge of the target nucleus and the number 16 is given in MeV/c and was determined by comparison with the exact result. Inclusion of this term with LEMA is referred to as LEMA + Δ . The electron mass has been neglected in comparison to

the electron momentum, so this approximation is not valid at extreme forward and backward electron scattering angles.

Previous workers [12,13] replaced the r -dependent momentum $p'(r)$ in Eq. (7) by the value $p'_{EMA} = p - V(0)$. This approximation is known as the Effective Momentum Approximation (EMA). Unfortunately, as we have known, the EMA describes the Coulomb effects on the wavefunction rather poorly [8,9]. Previous workers [12,13] also approximated the Coulomb phases by a constant plus a linear term in the operator \mathbf{J}^2 . While this approximation works well for low partial waves, it does not describe partial waves with angular momenta equal to or greater than pR where R is the nuclear radius. However, it is these partial waves that dominate inelastic electron scattering from the nucleus. We refer to the EMA plus linear fit to the phases as EMA- κ^2 . We avoid this problem by fitting the exact partial wave phase shifts δ_κ , where κ is the Dirac quantum number, to an expansion in powers of κ^2 . Retaining terms of second order in κ^2 for kappa values up to approximately $3(pR)$, we fit the exact phases with the following equation,

$$\delta_\kappa = b_0 + b_2\kappa^2 + b_4\kappa^4. \quad (8)$$

Note that the eigenvalues of \mathbf{J}^2 are $j(j+1)$ which equals $\kappa^2 - \frac{1}{4}$.

We also investigated the expansion of the phase exponential in Eq. (6) into a power series carried out by previous workers [12,13] and concluded that an accurate description requires many terms. We chose instead to neglect the electron spin dependence of the phases and replace $J^2 + \frac{1}{4}$ by the angular momentum squared L^2 in the exponential phase term for both incoming and outgoing waves. Further, we replace L^2 by its classical value $(\mathbf{r} \times \mathbf{p}')^2$. With these two approximations, the approximate Coulomb wavefunction is given by

$$\Psi^{(\pm)}(\mathbf{r}) = \frac{p'(r)}{p} e^{\pm ib_0} e^{\pm ib_2(\mathbf{r} \times \mathbf{p}(r))^2} \times e^{\pm ib_4(\mathbf{r} \times \mathbf{p}(r))^4} e^{ia(\hat{p}'(r) \cdot \hat{r})(\mathbf{r} \times \mathbf{p}(r))^2} e^{i\mathbf{p}'(r) \cdot \mathbf{r}} u_p. \quad (9)$$

The merits of this approach are that our approximate distorted Coulomb wavefunctions have an analytic plane-wave-like form and the Coulomb distortion modifications do not depend

on the electron spin, but the wavefunctions do have $(\mathbf{r} \times \mathbf{p}'(r))^2$ terms in the exponential which carry information about the phase shifts. We will refer to this wavefunction as the approximate analytic Coulomb distorted wavefunction. Based on our investigations, it is a good representation of the exact partial wave solutions for radial coordinates out to about three or four nuclear radii.

Using a technique introduced by Knoll [11] which approximates the potential in terms of the source current we obtain the following approximate Møller-type potential corresponding to our approximate analytic Coulomb distorted wavefunction,

$$\begin{aligned}
A^\mu(\mathbf{r}) = & \frac{4\pi}{4p_i p_f \sin^2 \frac{\theta_e}{2}} e^{i(b_{0i} + b_{0f})} e^{i[b_{2i}(\mathbf{r} \times \mathbf{p}'_i(r))^2 + b_{4i}(\mathbf{r} \times \mathbf{p}'_i(r))^4]} \\
& \times e^{i[b_{2f}(\mathbf{r} \times \mathbf{p}'_f(r))^2 + b_{4f}(\mathbf{r} \times \mathbf{p}'_f(r))^4]} \\
& \times e^{i[a_i(\hat{r} \cdot \hat{p}_i(r))(\mathbf{r} \times \mathbf{p}'_i(r))^2 - a_f(\hat{r} \cdot \hat{p}_f(r))(\mathbf{r} \times \mathbf{p}'_f(r))^2]} \\
& \times e^{i\mathbf{q}'(r) \cdot \mathbf{r}} \bar{u}_f \gamma^\mu u_i.
\end{aligned} \tag{10}$$

The Knoll approach is discussed in detail in previous work [8,9] and is a good approximation for momentum transfers greater than about 350 MeV/c. In arriving at Eq. (10), we neglected spatial derivatives of the phase factors in the wavefunction and the radial derivative of the local effective momenta $\mathbf{p}'(r)$.

The comparison of the approximate four potentials with the DWBA four potential requires a partial wave expansion since that is the only way the DWBA results can be obtained. However, the partial wave expansion for these potentials is hardly possible because of the $(\mathbf{r} \times \mathbf{p}')^2$ terms in the exponential. Traini *et al.*, [13] expanded the exponential in a power series up to the second order so as to use partial waves, but this series converges very slowly because the value of the phase, $b(\mathbf{r} \times \mathbf{p})^2$, is greater than one for regions of space near the nuclear surface. Of course, the origin of our approximations was in a partial wave formalism, so we can go back to that formalism and replace the exact phases and radial wavefunctions by the approximate phases and wavefunctions to obtain a measure of the quality of our approximations. Note, however, that obtaining the plane-wave-like form required some additional approximations including assuming that the asymptotic momentum transfer \mathbf{q} and

the phase factors in the approximate four potential do not explicitly depend on the incoming and outgoing electron spins.

With this caveat, we can compare various approximate potentials that have been widely used [12,13] and our approximate potential for selected multipoles. Figs. (1) and (2) show the comparison of two scalar potentials with the DWBA scalar potential by using the partial waves for different multipole L values. The initial spin and the final spin of the electron are $s_i = s_f = 1/2$. The calculations have been done using a Fermi charge distribution of radius $R = 6.65$ fm, with total charge $Z = 82$ and the angular momentum $L = 5$ and 15. The initial electron energy is $E_i = 400$ MeV, the final electron energy is $E_f = 300$ MeV, and the momentum transfer is $q = 350.5$ MeV/c. The solid line is the result for the DWBA scalar potential, the dotted line is for the $EMA - \kappa^2$ potential, and the dashed line is for our approximate potential of Eq. (10). The approximation for $EMA - \kappa^2$ has a different magnitude and is also out of phase, but that for our approximate potential almost has the same magnitude and is in phase. The discrepancy at large radii is due to lack of complete convergence of the κ series in the DWBA calculation and does not play an important role in calculating the cross section since the bound nucleon wavefunction drops very rapidly with radial distance. We conclude that our approximate potential is in quite good agreement with the exact potential calculated with partial waves (DWBA) for radial coordinates less than three to four nuclear radii, and hence is good enough to replace the full DWBA calculation. We have confirmed with the aid of a simple model [9] that our approximate potential reproduces the cross section calculated with the full partial wave result from DWBA quite well. We will show more realistic comparisons in the following sections that do not utilize a multipole decomposition and therefore is a more direct test of the approximate Coulomb distorted potential given in Eq. (10).

III. APPROXIMATE COULOMB DISTORTED CROSS SECTION

Using the approximate Møller potential given in Eq. (10) it is straightforward to derive the cross sections for $(e, e'p)$ reactions from nuclei since apart from the modified spatial dependence the approximate potential has the same Dirac structure as the plane wave Møller potential. The result is

$$\begin{aligned} \frac{d^3\sigma}{dE_f d\Omega_f d\Omega_P} &= \frac{PE_P}{(2\pi)^3} \sigma_M [v_L R'_L + v_T R'_T + \cos 2\phi_P v_{TT} R'_{TT} \\ &+ \cos \phi_P v_{LT} R'_{LT} + h \sin \phi_P v_{LT'} R'_{LT'}]. \end{aligned} \quad (11)$$

The electron structure functions are unchanged from Eq. (2), but the nuclear structure functions, designated with a prime superscript, contain Coulomb distortion effects. They are defined as in Eqs. (3) and (4), except that the ‘‘Fourier’’ transforms given in Eq. (5) become

$$\begin{aligned} N'_0 &= \int \left(\frac{q'_\mu(r)}{q_\mu}\right)^2 \left(\frac{q}{q'(r)}\right)^2 e^{i(\delta_i + \delta_f + \Delta_i - \Delta_f)} J_0 e^{i\mathbf{q}'(r)\cdot\mathbf{r}} d^3r \\ N'_{x,y} &= \int e^{i(\delta_i + \delta_f + \Delta_i - \Delta_f)} J_{x,y} e^{i\mathbf{q}'(r)\cdot\mathbf{r}} d^3r, \end{aligned} \quad (12)$$

where the phase shift δ and the ad-hoc additional phase Δ are functions of \mathbf{r} given by

$$\begin{aligned} \delta &= b_0 + b_2(\mathbf{r}\times\mathbf{p}'(r))^2 + b_4(\mathbf{r}\times\mathbf{p}'(r))^4 \\ \Delta &= a(\hat{r}\cdot\hat{p}(r))(\mathbf{r}\times\mathbf{p}'(r))^2. \end{aligned} \quad (13)$$

The result in Eq. (11) is our primary finding. Our approximate treatment of Coulomb distortion leads to a ‘‘plane-wave-like’’ form for the cross section and thereby opens up the possibility of investigating the various ‘‘structure functions’’ independently. Of course, these more generalized ‘‘structure functions’’ do contain some dependence on the electron kinematics, but with the use of theoretical nuclear models, this modification of the structure functions can be investigated.

The charge transform in Eq. (11) differs from the transverse current transforms since the continuity equation was used to eliminate the z-component of the current. Note that

unlike the case for electron plane waves, the various current transforms are not azimuthally symmetric about the momentum transfer direction \mathbf{q} , and therefore contain dependencies on the outgoing nucleon azimuthal angle ϕ_P over and beyond the explicit dependencies shown in Eq. (11). However, some symmetry remains since both $(\mathbf{r} \times \mathbf{p}_i'(r))^2$ and $(\mathbf{r} \times \mathbf{p}_f'(r))^2$ are invariant under the transformation $\phi \rightarrow -\phi$ which results in the nuclear structure being invariant under $\phi_P \rightarrow -\phi_P$. The consequences of this additional dependence on ϕ_P will be discussed further in the next section.

IV. RESULTS

A. Cross section in parallel and perpendicular kinematics

In our analysis we are looking at one particular shell, and trying to find the reduced cross section ρ_m , which for proton waves in the final state is related to the probability that a bound proton from a given shell with the missing momentum \mathbf{p}_m can be knocked out of the nucleus with asymptotic momentum \mathbf{P} . The reduced cross section as a function of p_m is commonly defined by

$$\rho_m(p_m) = \frac{1}{PE_P\sigma_{eP}} \frac{d^3\sigma}{dE_f d\Omega_f d\Omega_P}, \quad (14)$$

where the missing momentum can be determined by the kinematics $\mathbf{p}_m = \mathbf{P} - \mathbf{q}$. The off-shell electron-proton cross section σ_{eP} is not uniquely defined, but in all cases we use the form σ_{eP}^{cc1} given by deForest [14].

There are two kinematical situations commonly used in $(e, e'p)$ experiments. They are parallel kinematics where the outgoing proton momentum \mathbf{P} is along the momentum transfer \mathbf{q} and perpendicular kinematics where the magnitude of \mathbf{P} is fixed, but the detected proton makes an angle θ_{Pq} with respect to \mathbf{q} . In perpendicular kinematics, the magnitude of \mathbf{P} is usually equal to the magnitude of \mathbf{q} . All calculations will be carried out in the laboratory frame (target fixed frame). In the parallel case, the three interference terms in Eq. (14) disappear, while in the perpendicular case, all terms remain except the fifth structure function

which sums to zero for unpolarized incoming electrons. Our approximate calculations for the $(e, e'p)$ reaction include the approximate phase factors and the correction term Δ by keeping the exponential form and the transition matrix element is evaluated by three dimensional integration since a multipole expansion is no longer practical. We compare our results to the full DWBA results [1,2] and the experimental data from NIKHEF [15,16] in Amsterdam. The electron incoming energy is given by $E_i = 412$ MeV and the ejected proton kinetic energy $T_P = 100$ MeV. All calculations include the proton final state interaction by using a relativistic optical potential obtained from fitting to elastic proton scattering data [7].

In Figs. (3) and (4), we show two results corresponding to knocking out a proton from a $3s_{1/2}$ shell and a $2d_{3/2}$ shell in ^{208}Pb for the case of parallel kinematics. For this kinematics, the proton momentum \mathbf{P} is parallel to the asymptotic momentum transfer \mathbf{q} which defines the $\hat{\mathbf{z}}$ axis and the missing momentum \mathbf{p}_m is also along the \mathbf{q} direction. The dotted line is the PWBA result obtained by using a multipole expansion and doing the one dimensional integration over r in the normal way, while the dash-dotted line uses the approximate potential with $Z=1$ evaluated by three dimensional numerical integration. They are in excellent agreement (to better than 1%) as they should be since the approximate calculations approaches the plane wave result as $Z \rightarrow 0$. The solid line is our approximate Coulomb distorted result obtained by numerical integration while the dashed line is the full DWBA results obtained by using partial waves and multipole analysis. The dash-three-dotted line is the $EMA - \kappa^2$ result also obtained by using three dimensional integration. The diamonds are data from NIKHEF. Note that the primary effect of Coulomb distortion is to shift the reduced cross section by about 20 MeV/c in missing momentum to the right as compared to the plane wave results. The approximate DWBA results reproduce the full DWBA results well around the first peak where the difference is less than 2%, but deviate somewhat for large missing momentum where the reduced cross section is smaller. The approximate DWBA result breaks down rapidly beyond missing momentum $p_m = 100$ MeV/c on the right side, but since $\mathbf{q} = \mathbf{P} - \mathbf{p}_m$, positive p_m corresponds to small q and we expect our approximation to become worse for q less than about 350 MeV/c as discussed in Section 2.

The $EMA - \kappa^2$ result is lower by about 30% around the first peak than the full DWBA result. Note further that the electron distortion affects the positive missing momentum p_m and the negative p_m differently. The negative p_m region shows a large Coulomb distortion effect. Figs. (5) and (6) show the reduced cross sections from $3s_{1/2}$ and $2d_{3/2}$ for ^{208}Pb for perpendicular kinematics. We choose $\mathbf{P} = \mathbf{q}$ which marks the top of the quasielastic peak for s-states. The electron angle corresponding to this momentum transfer is $\theta_e = 74^\circ$ for $E_i = 412$ MeV and the ejected proton energy $T_P = 100$ MeV. The dotted line is the PWBA result, the solid line is our approximate result, the dash-three-dotted line is the $EMA - \kappa^2$ result, and the dashed line is the full DWBA result. Since the momentum transfer is large, $q = 444$ MeV/c, the approximate results are in much better agreement with the full DWBA results than those of the parallel kinematics case discussed above. The difference is less than 2% around the first peak as in the parallel case, and for both side regions the deviation is around 5%. The positions of the maxima and minima are in the right places. The discrepancy between the DWBA result and the $EMA - \kappa^2$ result is greater than 30% around the first peak. These results confirm previous observations that Coulomb distortion has smaller effects in perpendicular kinematics than in parallel kinematics.

From these calculations of two different kinematic cases for the $(e, e'p)$ reaction, the approximate DWBA results reproduce the full DWBA and the experimental results quite well, especially around the first peak. The effect of the Coulomb distortion on the cross section for a knocked-out proton from the $3s_{1/2}$ shell for ^{208}Pb is almost 30% but that for knocked-out from the $2d_{3/2}$ shell is only 10% as compared to the PWBA calculation.

In the past, $(e, e'p)$ experiments in parallel kinematics have been measured for the reduced cross section in the missing momentum range $-50 \leq p_m \leq 300$ MeV/c at NIKHEF. Recently, the range of the missing momentum has been extended to $300 \leq p_m \leq 500$ MeV/c by $(e, e'p)$ measurements for perpendicular kinematics [17]. The new reduced cross section was measured at momentum transfer $q = 221$ MeV/c, energy transfer $\omega = 110$ MeV, the kinetic energy of the detected proton $T_p = 100$ MeV, and incident electron energy $E_i = 487$ MeV as shown in Fig. (7). The dotted line is the PWBA result, the solid line is our ap-

proximate DWBA result, and the diamonds are the experimental data from NIKHEF [17]. Our result reproduces the measured reduced cross section very well although the momentum transfer q is small. A similar conclusion has been drawn [19] by the Madrid group using their DWBA calculation to analyse this same data. The interesting physics point is that our “single-particle” relativistic model reproduces the experimental data at large missing momentum quite well and should be compared to an analysis of this same reaction with a non-relativistic approach which uses a non-relativistic current operator and finds it necessary to introduce many different two-body currents to even come close to the data [18]. It should be noted that our calculation only contains one free parameter, the spectroscopic factor which is an overall scale factor of 0.71 which had already been determined [1]–[4] by the low missing momentum data.

B. Interference Structure Functions

In previous work [4], the effect of Coulomb distortion on the magnitude of the fourth structure function was more than 15% in ^{16}O , and more than a factor of 2 in ^{208}Pb . The magnitude effect on the fifth structure function depends on the out-of-plane angle of the knocked out proton used in the extraction and was more than 15% for a small angle (e.g. 10°) data in ^{16}O . Since the structure functions appear in the cross section with different electron kinematic factors, one can study them independently, but we will show below that the PWBA formalism is no longer valid in the presence of the static Coulomb field of the nucleus. Even though the separation for the full DWBA calculation with a partial wave expansion is not valid in the presence of the Coulomb distortion, it is possible to calculate the fourth and the fifth structure functions which embody left-right and up-down asymmetries of the cross section measured with respect to the momentum transfer direction. We call a quantity so determined the *apparent* structure function, and note that it would correspond to a structure function extracted from experiment. In our model, we can also directly calculate the “structure functions” as given by Eq. (3) when the distorted “Fourier”

transforms of Eq. (12) are used. One question is to what extent these two results agree with each other.

From Eq. (1) one can see that the fourth structure function R_{LT} could be obtained experimentally by subtracting the cross sections with $\phi_P = 0$ and $\phi_P = \pi$ while keeping other electron and proton kinematic variables fixed. The fourth apparent structure function determined by the left-right asymmetry with respect to the momentum transfer direction is given by

$$R_{LT}^a = \frac{\sigma^L - \sigma^R}{2Kv_{LT}} \quad (15)$$

where L (left) indicates $\phi_P = 0$ and R (right) indicates $\phi_P = \pi$. The constant $K = \frac{PE_P}{2\pi^3}\sigma_M$ and the electron structure functions v are defined in Eq. (2). The superscript a means the apparent structure function including the electron Coulomb distortion, and corresponds to what one would extract from experiment. If the incoming electron beam is polarized ($h = 1$), one can extract the apparent fifth structure function by the up-down asymmetry of the cross section given by

$$R_{LT'}^a = \frac{\sigma^U - \sigma^D}{2Kv_{LT'}\sin\phi_P} \quad (16)$$

where U (up) means $0 < \phi_P < \pi$ (above the plane) and D (down) means $-\phi_P$ (below the plane).

We extract the fourth structure functions for the $3s_{1/2}$ orbit of ^{208}Pb with incident electron energy $E_i = 500$ MeV as shown Fig. (8). The dotted line and the dashed line are the fourth structure functions calculated directly using Eq. (12) for the PWBA and the approximate DWBA result, while the dash-dotted line, the solid line, and the dash-three-dotted line are the apparent fourth structure functions from Eq. (15) for the PWBA, the approximate DWBA and the full DWBA calculation, respectively. We compared our approximate DWBA calculation of the cross section to the full DWBA and found the difference to be less than 2% around the first peak, and around 5% at the second peak. When Coulomb distortion is included the directly calculated fourth structure function differs from the apparent fourth

structure function by a factor of 3 at the peaks. Of course for the PWBA calculation the apparent fourth structure function agrees exactly with the directly calculated fourth structure function. Clearly, the standard separation formalism is no longer valid in the presence of the electron Coulomb distortion for the fourth structure function R_{LT} . Furthermore, while the effect of the electron Coulomb distortion is on the order of 30% for the cross section, it changes the apparent fourth structure function by more than a factor of 2.

In Fig. (8) the discrepancy between the directly calculated fourth structure function R'_{LT} and the apparent fourth structure function for the approximate DWBA suggests that the structure functions depend on the azimuthal angle of the ejected proton as expected. In order to reduce this dependence, we investigated changing the definition of the $\hat{\mathbf{z}}$ axis, normally defined by asymptotic momentum transfer \mathbf{q} , in order to bring the apparent and direct structure functions into closer agreement. We considered two choices, one where $\hat{\mathbf{z}}$ is taken to lie along $\mathbf{q}'(R) = \mathbf{p}'_i(R) - \mathbf{p}'_f(R)$ where $p'(R) = p - V(R)$ and $V(R)$ is the value of the Coulomb potential at the nuclear surface, and the second along $\mathbf{q}'(0) = \mathbf{p}'_i(0) - \mathbf{p}'_f(0)$ where $p'(0) = p - V(0)$ and $V(0)$ is the Coulomb potential at the origin. The second case corresponds to the EMA approximation. We carried out our approximate DWBA calculations for both choices and show the results for the $3s_{1/2}$ orbit of ^{208}Pb in Fig. (9). The incident electron energy $E_i = 500$ MeV, the proton kinetic energy $T_p = 100$ MeV, and the outgoing proton momentum is equal to the momentum transfer q . The solid line is the directly calculated R'_{LT} and the dotted line is the apparent fourth structure function obtained when $\hat{\mathbf{z}}$ is along $\mathbf{q}'(R)$. The dashed line is the directly calculated R'_{LT} and the dash-dotted line is the apparent fourth structure function obtained by using $\mathbf{q}'(0)$ to define the $\hat{\mathbf{z}}$ axis.

When choosing the $\hat{\mathbf{z}}$ axis along $\mathbf{q}'(0)$, the apparent structure function is out of phase with the direct structure function and the magnitude is suppressed at the first peak, but by using the $\hat{\mathbf{z}}$ axis along $\mathbf{q}'(R)$ the structure functions are in phase and the magnitudes are quite close. Thus, changing the $\hat{\mathbf{z}}$ axis to be along the direction of $\mathbf{q}'(R)$ permits the extraction of a fourth structure function R'_{LT} . Furthermore, choosing this different $\hat{\mathbf{z}}$ axis largely removes

the Coulomb distortion effects on the fourth structure function, at least around the first peak. From these results, we recommend that one can experimentally extract the fourth structure function by choosing the $\hat{\mathbf{z}}$ axis along the new modified momentum transfer $\mathbf{q}'(R)$. Note that θ_P of the ejected proton in these plots is the polar angle measured from the differently chosen $\hat{\mathbf{z}}$ axes.

Using a polarized incident electron beam and detecting the knocked out proton out of the scattering plane, the fifth structure function $R'_{LT'}$ can be extracted by measuring the up-down asymmetry of the nuclear response. We also choose the incident electron energy $E_i = 500$ MeV, the proton kinetic energy $T_P = 100$ MeV, and the momentum transfer q equal to the proton momentum p for this case.

We first look at the Coulomb distortion effect on the measurement of the fifth structure function from the $3s_{1/2}$ orbit of ^{208}Pb at fixed proton azimuthal angle $\phi_P = 40^\circ$ as shown Fig. (10). The direct fifth structure function again agrees with the apparent structure function in PWBA calculation as expected. The dotted line is the fifth structure function for the PWBA, and the solid line is the fifth structure function with the $\hat{\mathbf{z}}$ axis along the asymptotic momentum \mathbf{q} and the dashed line is for the case of the $\hat{\mathbf{z}}$ axis along the modified momentum transfer $\mathbf{q}'(R)$. We confirmed that the direct fifth structure function agrees with the apparent structure function for the approximate DWBA calculation as expected from our earlier observation that the approximate structure functions are symmetric under the transformation $\phi_P \rightarrow -\phi_P$. Thus when one calculates $\sigma^U - \sigma^D$ all other terms cancel leaving only the $R'_{LT'}$ contribution. Note that unlike the case for R'_{LT} , changing the $\hat{\mathbf{z}}$ axis does not affect the shape and magnitude and does not reduce the Coulomb distortion effect significantly. Thus, one can experimentally extract a fifth structure function without redefining the $\hat{\mathbf{z}}$ axis. Of course, Coulomb distortion clearly affects the magnitude of $R'_{LT'}$ as compared to the plane wave result (by approximately 30% for ^{208}Pb).

In Fig. (11), we show the fifth structure function as a function of ϕ_P at fixed polar proton angles, $\theta_P = 4^\circ$, for the $3s_{1/2}$ orbit of ^{208}Pb and the $1s_{1/2}$ orbit of ^{16}O , and $\theta_P = 14^\circ$ for the $1p_{1/2}$ orbit of ^{16}O . These polar angles are the first peak position of the fifth structure function

for the $s_{1/2}$ orbit of ^{208}Pb and the $p_{1/2}$ orbit of ^{16}O respectively for these kinematics. The dotted line is the PWBA result and the solid line and the dashed line are the approximate DWBA results obtained by choosing the $\hat{\mathbf{z}}$ axis along the asymptotic momentum transfer \mathbf{q} and along the momentum transfer $\mathbf{q}'(R)$. The approximate DWBA calculation for the $p_{1/2}$ orbit of $^{16}\text{O}(e, e'p)$ in Fig. (11) reproduces the same shape as the full DWBA calculation [4] for the fifth structure function, but both differ in magnitude from the plane wave result. In this previous paper [4] where the full DWBA calculation was applied to a particular case, it was concluded that extracting the fifth structure function $R_{LT'}$ at $\phi_P = 90^\circ$ or averaging over ϕ_P largely removed the Coulomb distortion effects. Clearly that is not the case here. Therefore, it is not true in general that the Coulomb distortion effect can be removed at $\phi_P = 90^\circ$. Furthermore, we again note that choosing a different $\hat{\mathbf{z}}$ axis does not help in removing the Coulomb effect for the fifth structure function unlike the case of the fourth structure function. We also confirmed that the fifth structure function extracted by using the incident electron helicity dependence or the up-down asymmetry agree exactly as expected from the $\phi_p \rightarrow -\phi_p$ symmetry discussed earlier in the approximate Coulomb distorted form factors.

V. CONCLUSIONS

We have developed a plane-wave-like approximate solution to the Dirac equation in the presence of the static Coulomb field of a nucleus which agrees rather well with the exact partial wave solutions inside a sphere of approximately three times the nuclear radius. The limited spatial range of the approximation is not a serious restriction for electron induced nuclear processes since the bound state wavefunctions that enter any such process drop off exponentially outside the nuclear radius R . Using this approximate wavefunction, along with a few additional approximations, we also obtained an approximate DWBA potential valid for momentum transfers greater than about 350 MeV/c. This approximate potential has the same Dirac structure as the plane wave Møller potential although it contains some

spatially dependent phase factors which destroy the azimuthal spatial symmetry about the momentum transfer direction \mathbf{q} . The basic ingredients in our approximate potential are the static Coulomb potential of the target nucleus and the elastic scattering phase shifts for the incoming and outgoing electron energies in this potential.

We have compared wavefunctions, potentials and cross sections for the $(e, e'p)$ reaction on nuclei in the quasielastic region calculated with our approximation and previous approximations to the exact partial wave results. We find that the previous approximate results are in serious disagreement with the exact partial wave results. Our approximate results are in good agreement with the full DWBA results, but have a number of advantages over the DWBA results. The biggest advantage is that the plane-wave-like structure of the approximate Coulomb distorted potential allows extraction of structure functions which are bi-linear products of transforms of the transition current components. However, unlike the PWBA analysis, these transforms are not just Fourier transforms, but contain additional spatial dependence on the kinematics resulting from the static Coulomb field of the target nucleus.

In this paper, we investigated in some detail the extraction of the so-called fourth structure function R'_{LT} and fifth structure function $R'_{LT'}$ from the full cross section. We showed that this is possible, particularly for kinematics where the structure functions are large. However, for the case of the fourth structure function, R'_{LT} , the $\hat{\mathbf{z}}$ axis needs to be redefined to lie along the momentum transfer defined at the nuclear surface $\mathbf{q}'(R) = \mathbf{p}'_i(R) - \mathbf{p}'_f(R)$ to obtain agreement between the directly calculated structure function and the extracted structure function. For the fifth structure function $R'_{LT'}$, there is no need to redefine the $\hat{\mathbf{z}}$ axis.

The other major advantage of our approximate treatment of Coulomb distortion over the full DWBA partial wave calculation is that it is straightforward to apply it to higher energies. The full DWBA calculation at higher electron energies requires more and more partial waves with increasingly forbidding amounts of computer time needed. Using our approximate treatment, we do find it necessary to perform two additional numerical integrations over

angular coordinates θ and ϕ in the interaction matrix element as compared to a treatment that permits a multipole decomposition. However, these numerical integrations are not very time consuming and in a sense are just a replacement for summing over various intermediate angular momenta arising from angular momentum recoupling of the various partial wave expansions of the wavefunction and transition matrix elements. In our particular case, we have an analytic result for the electromagnetic potential so that the three dimensional integration is very fast as compared to a full partial wave analysis and the evaluation of thousands of radial matrix elements.

In conclusion, our approximate treatment of Coulomb distortion for electron induced nuclear processes involving continuum nucleons works quite well and is particularly good for momentum transfers greater than 350 MeV/c. It permits the extraction of "structure functions" which should prove of great use in analysing $(e, e'p)$ experiments at the Thomas Jefferson National Accelerator Facility and other laboratories. Of course, it is an approximation and if one has very high precision data it may be necessary to revert to the full DWBA calculation.

ACKNOWLEDGMENTS

We thank the Ohio Supercomputer Center in Columbus for many hours of Cray Y-MP time to develop this calculation and to perform the necessary calculations. This work was supported in part by the U.S. Department of Energy under Grant No. FG02-87ER40370.

FIGURES

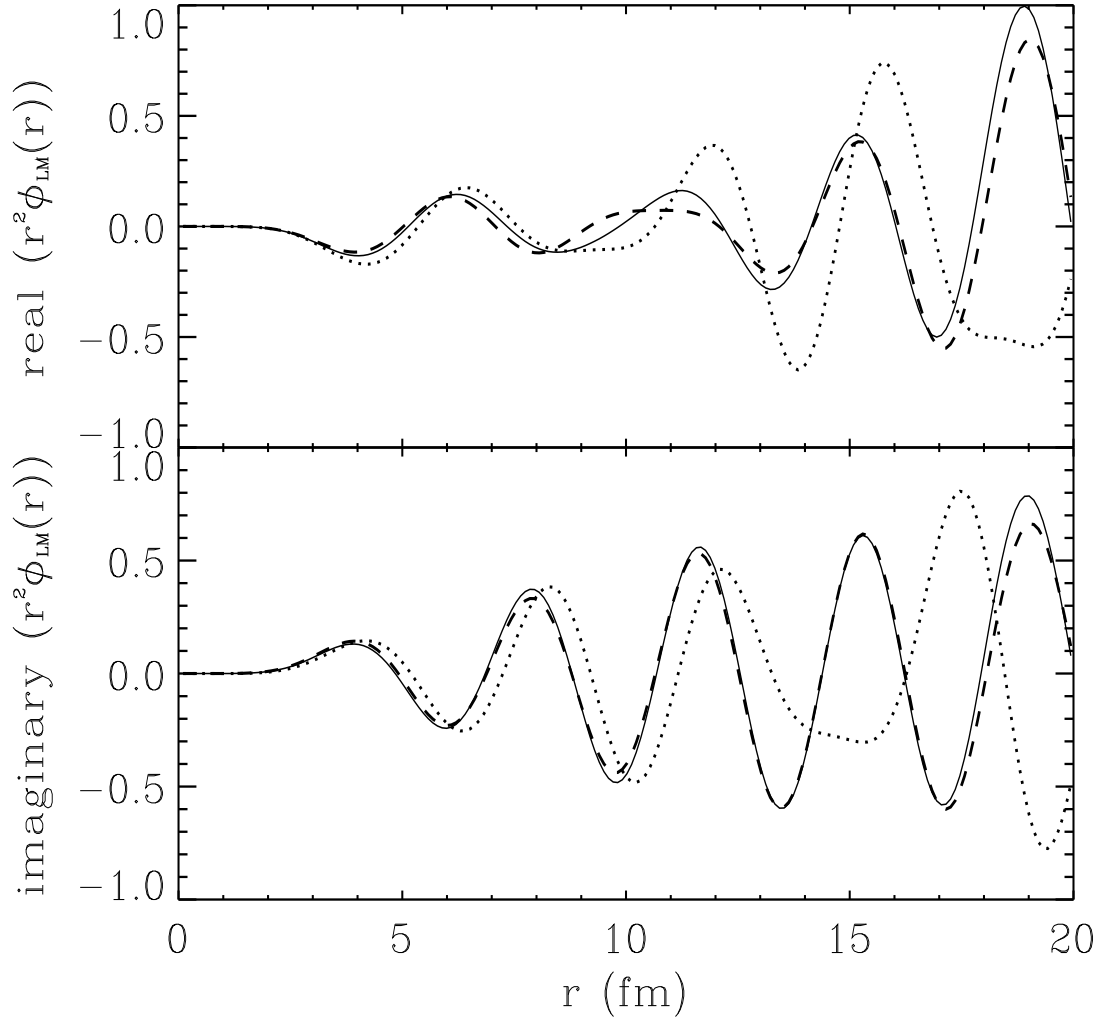


FIG. 1. Comparison of the exact scalar potential with approximate scalar potentials for the multipole component $L=5$, $M=0$. The initial energy $E_i = 400$ MeV and the energy loss $\omega = 100$ MeV. The solid line is calculated with DWBA, the dotted line with $EMA - \kappa^2$ and the dashed line is our approximate potential.

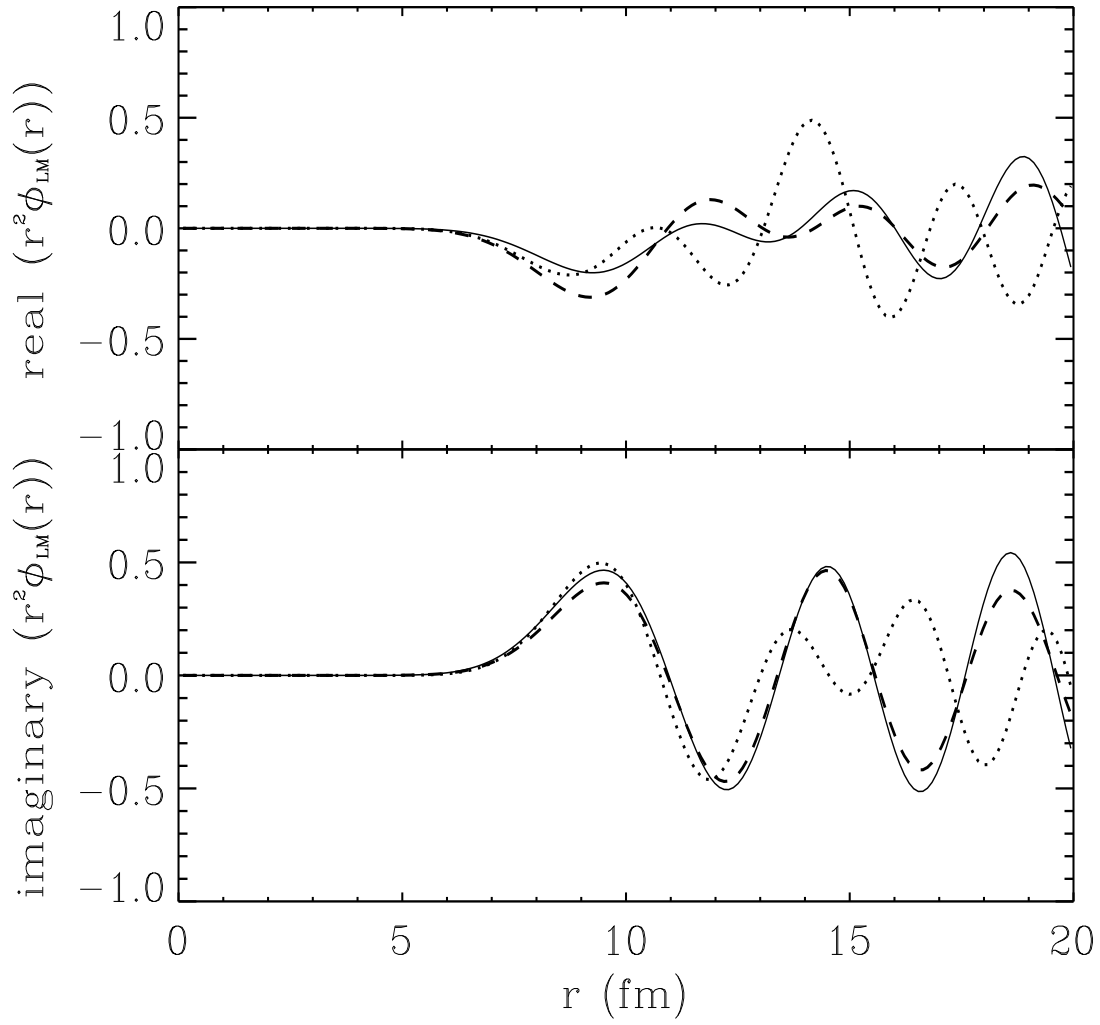


FIG. 2. The same as Fig. (1) with multipole $L = 15$ and $M = 0$.

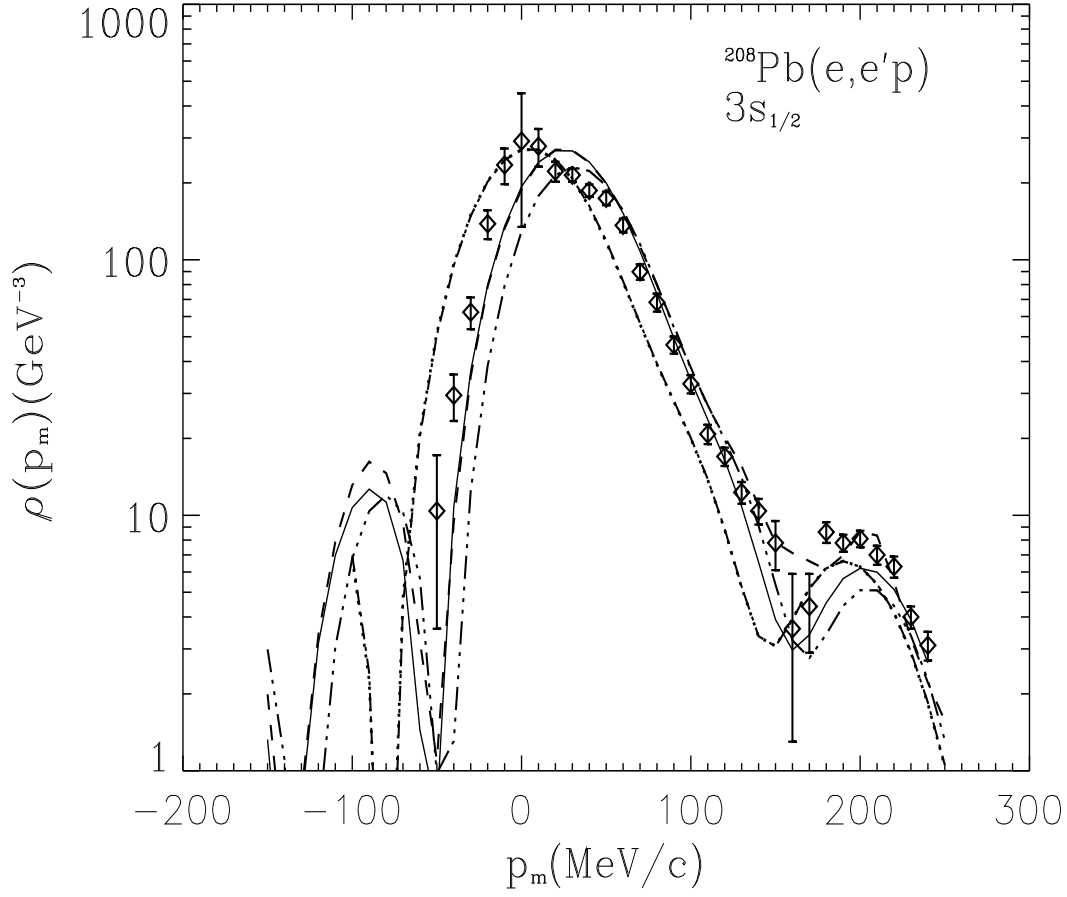


FIG. 3. Reduced cross sections for $^{208}\text{Pb}(e, e'p)$ from the $3s_{1/2}$ shell with parallel kinematics. The kinematics are $E_i = 412$ MeV, and proton kinetic energy $T_P = 100$ MeV. The dotted line is the PWBA result and the dash-dotted line (which falls on top of it) is the approximate DWBA result with $Z = 1$. The dash-three-dotted line is the $EMA - \kappa^2$ result, the solid line is the approximate DWBA result, the dashed line is the full DWBA result, and the diamonds are data from NIKHEF. The same spectroscopic factor of 71% is used in all curves.

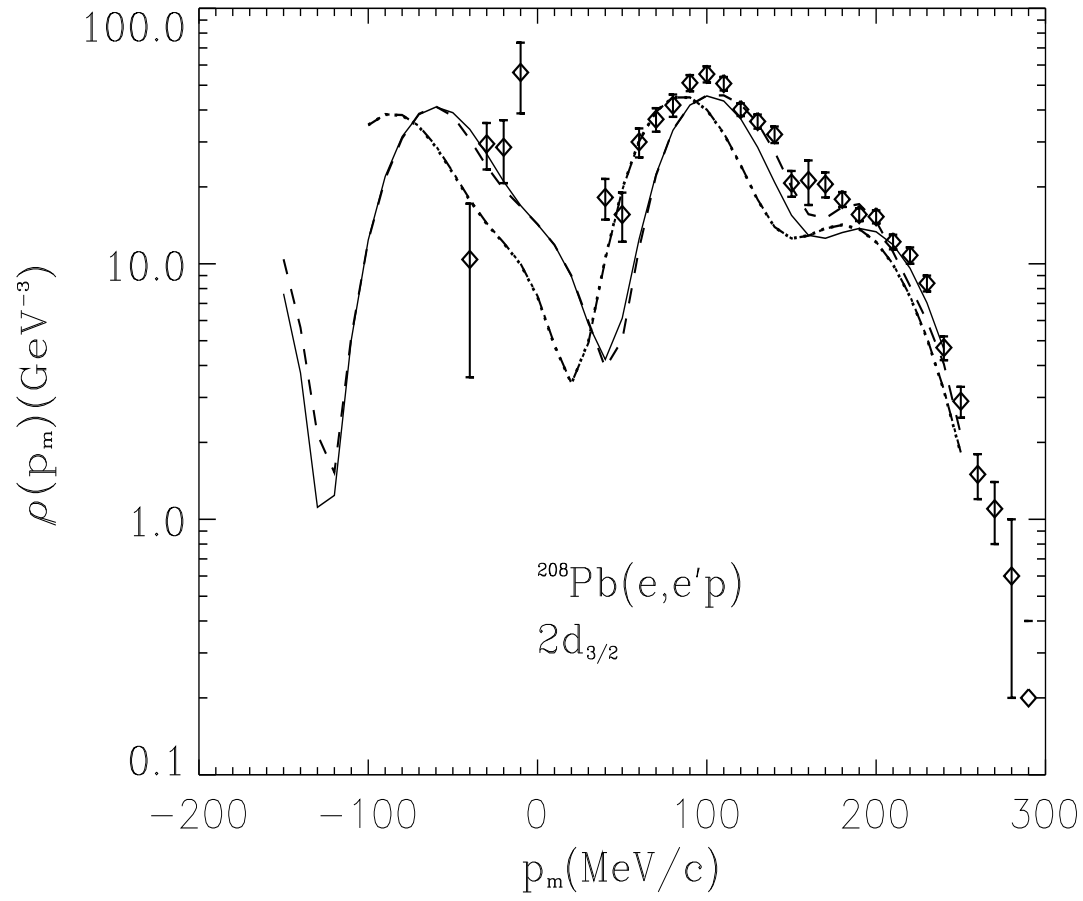


FIG. 4. The same as Fig. (3) except for the $2d_{3/2}$ shell and the $EMA - \kappa^2$ result is not shown.

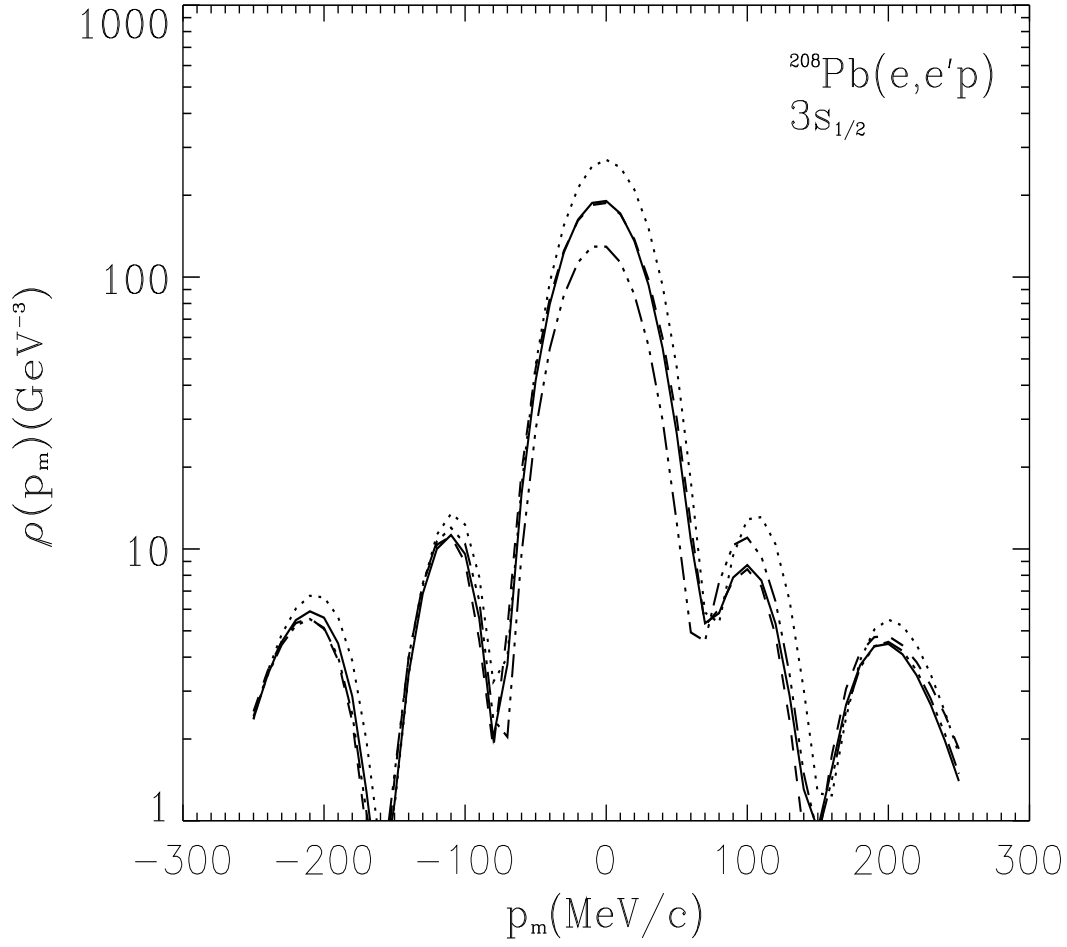


FIG. 5. Reduced cross sections for $^{208}\text{Pb}(e, e'p)$ from the $3s_{1/2}$ shell with perpendicular kinematics. The kinematics are $E_i = 412$ MeV, and proton kinetic energy $T_P = 100$ MeV. The dotted line is the PWBA result, the dash-three-dotted line is the $EMA - \kappa^2$ result, the solid line is our approximate result, and the dashed line is the full DWBA result.

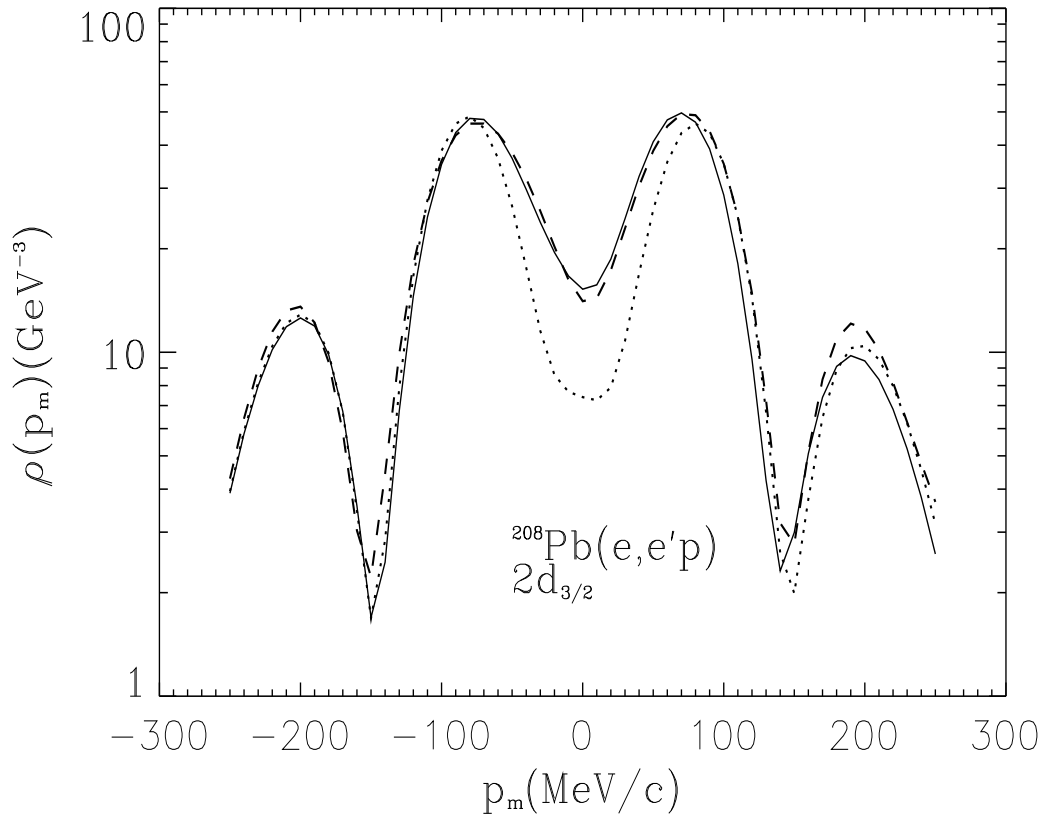


FIG. 6. The same as Fig. (5) except the $2d_{3/2}$ shell.

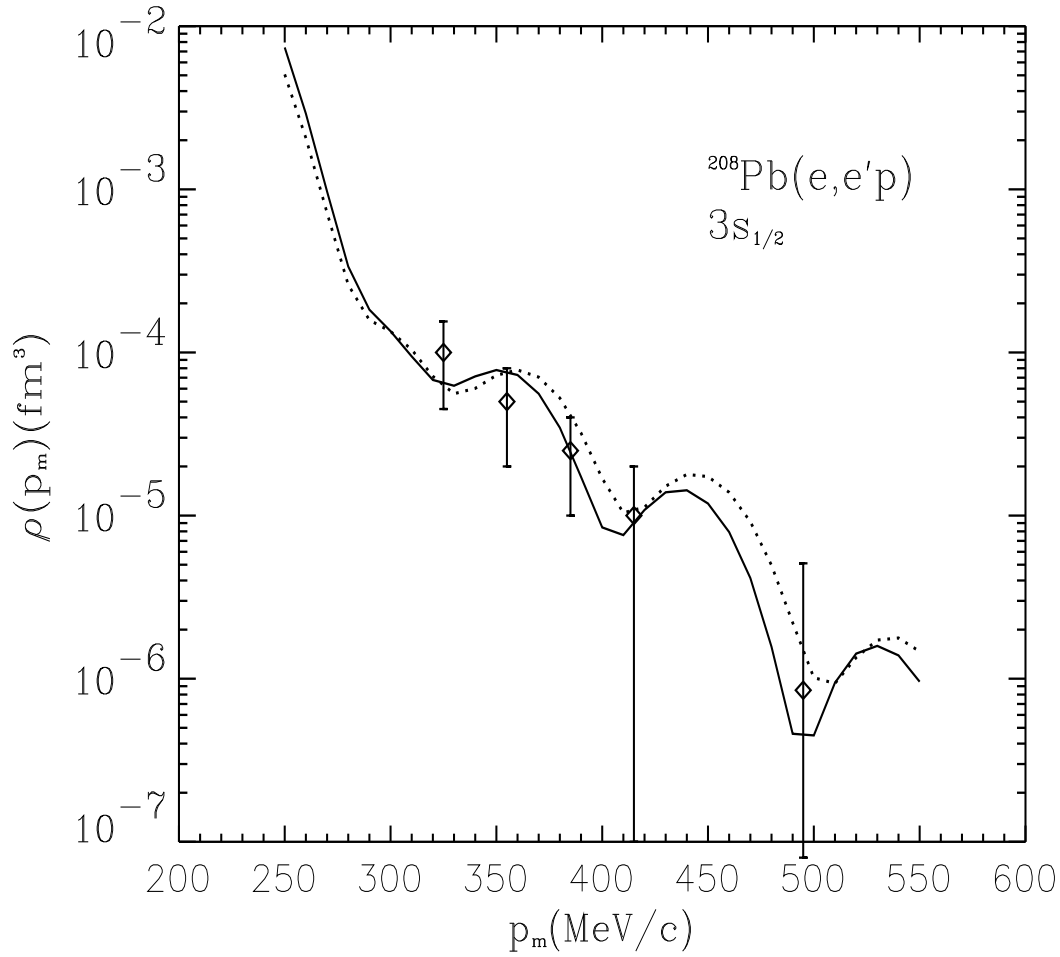


FIG. 7. Reduced cross sections for $^{208}\text{Pb}(e, e'p)$ from the $3s_{1/2}$ shell for high missing momentum. The kinematics are $E_i = 487$ MeV, momentum transfer $q = 221$ MeV/c, energy transfer $\omega = 110$ MeV, and proton kinetic energy $T_P = 100$ MeV. The solid line is the approximate DWBA result, the dotted line is the PWBA result, and the diamonds are data from NIKHEF. A previously determined spectroscopic factor of 71% was used for both curves.

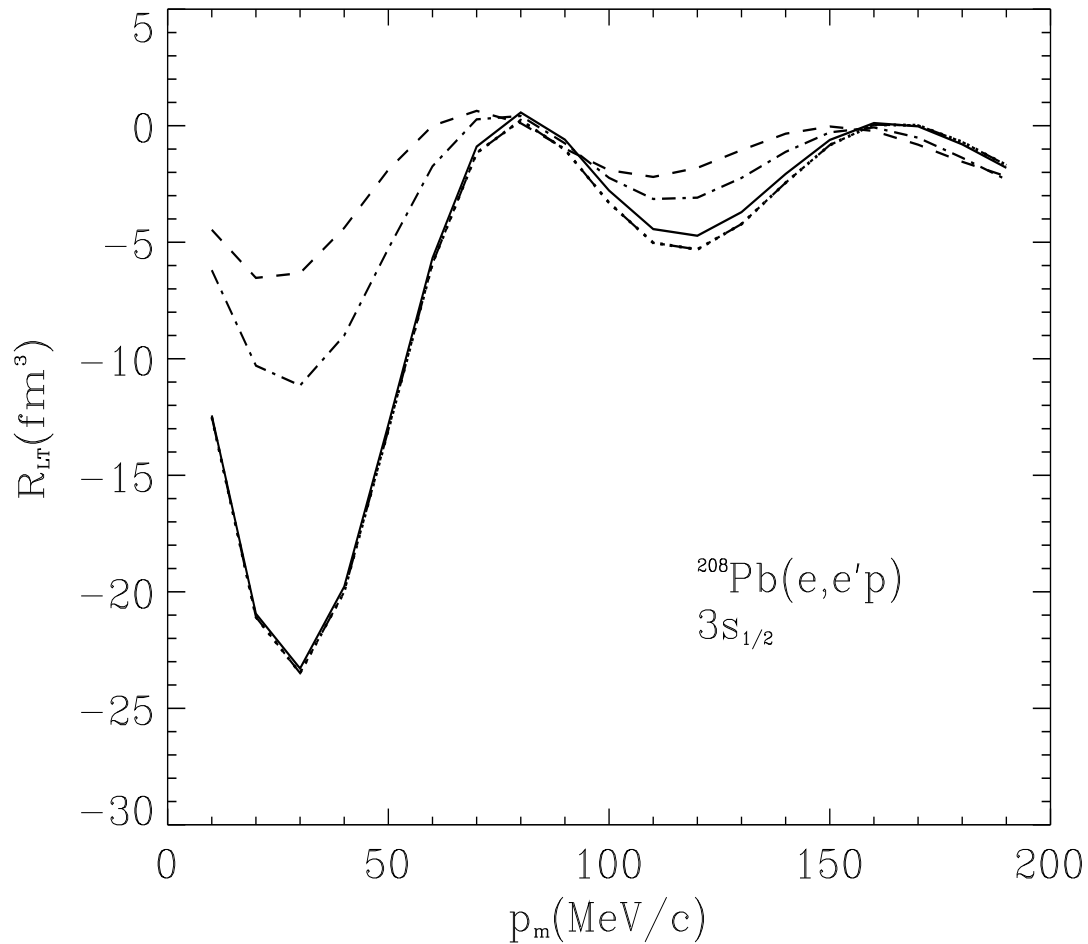


FIG. 8. The fourth structure function for $^{208}\text{Pb}(e, e'p)$ from the $3s_{1/2}$ shell as a function of missing momentum. The kinematics are $E_i = 500$ MeV, and proton kinetic energy $T_P = 100$ MeV. The dash-dotted line is the apparent structure function and dotted line is the directly calculated structure function for the PWBA (which fall on top of each other). The solid line is the apparent and the dashed line is the directly calculated structure function for the approximate DWBA result, while the dash-three-dotted line is the apparent structure function for the full DWBA result.

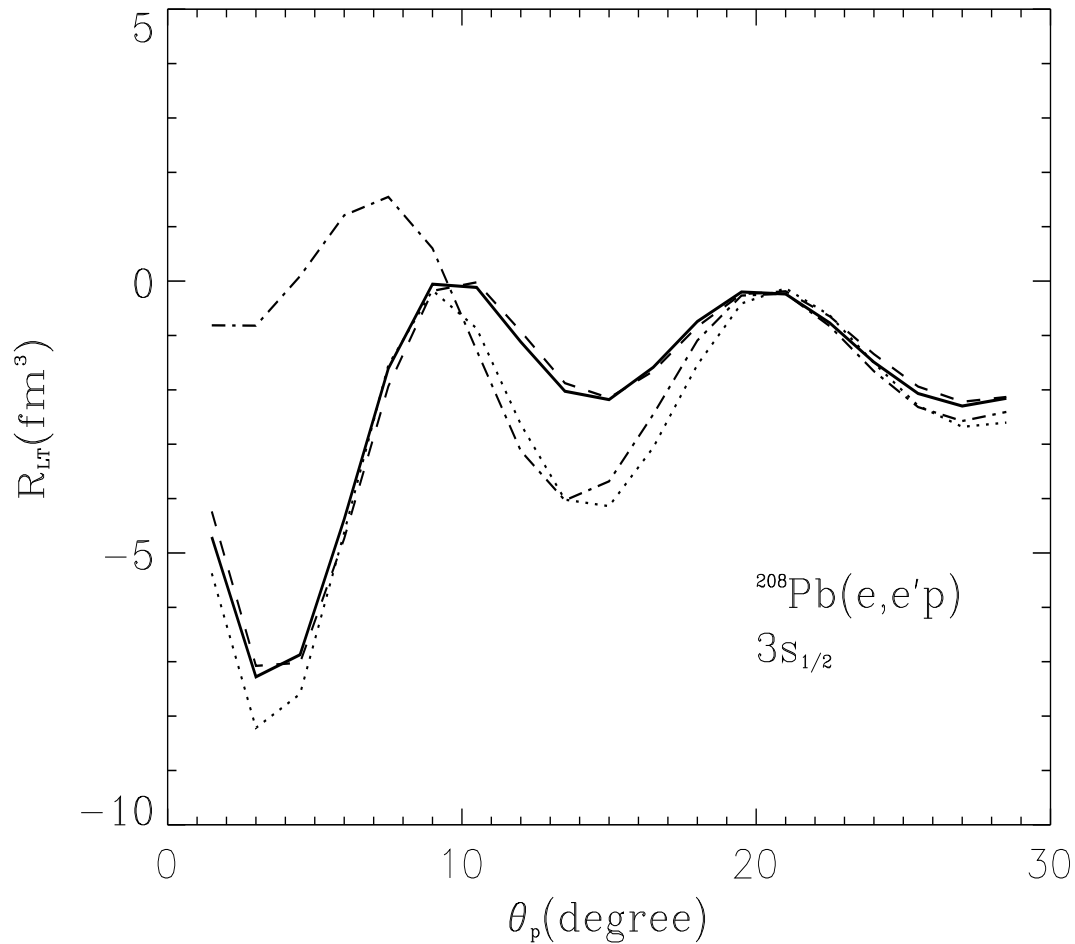


FIG. 9. The fourth structure function for $^{208}\text{Pb}(e, e'p)$ for the $3s_{1/2}$ orbit as a function of the polar angle of the ejected proton. The solid line and the dotted line are the direct and the apparent structure function with the $\hat{\mathbf{z}}$ axis along the momentum transfer $\mathbf{q}'(R)$, and the dashed line and the dash-dotted line are the direct and the apparent structure function for the case of the $\hat{\mathbf{z}}$ axis along the EMA momentum $\mathbf{q}'(0)$.

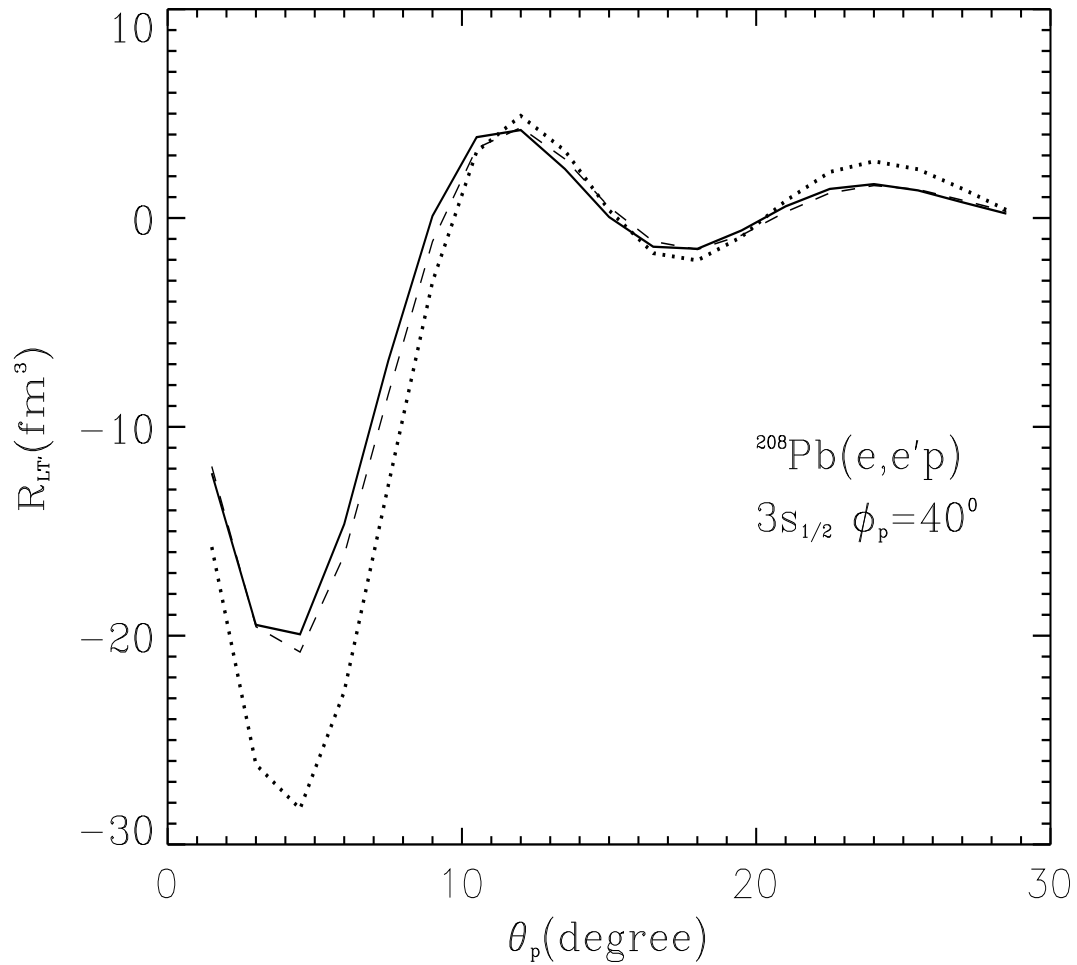


FIG. 10. The fifth structure function for $^{208}\text{Pb}(e, e'p)$ from the $3s_{1/2}$ shell as a function of the polar angle of the ejected proton. The dotted line is the fifth structure function for the PWBA, while the solid and the dashed lines are approximate DWBA results with the \hat{z} axis along the asymptotic momentum \mathbf{q} and along the modified momentum transfer $\mathbf{q}'(R)$ respectively.

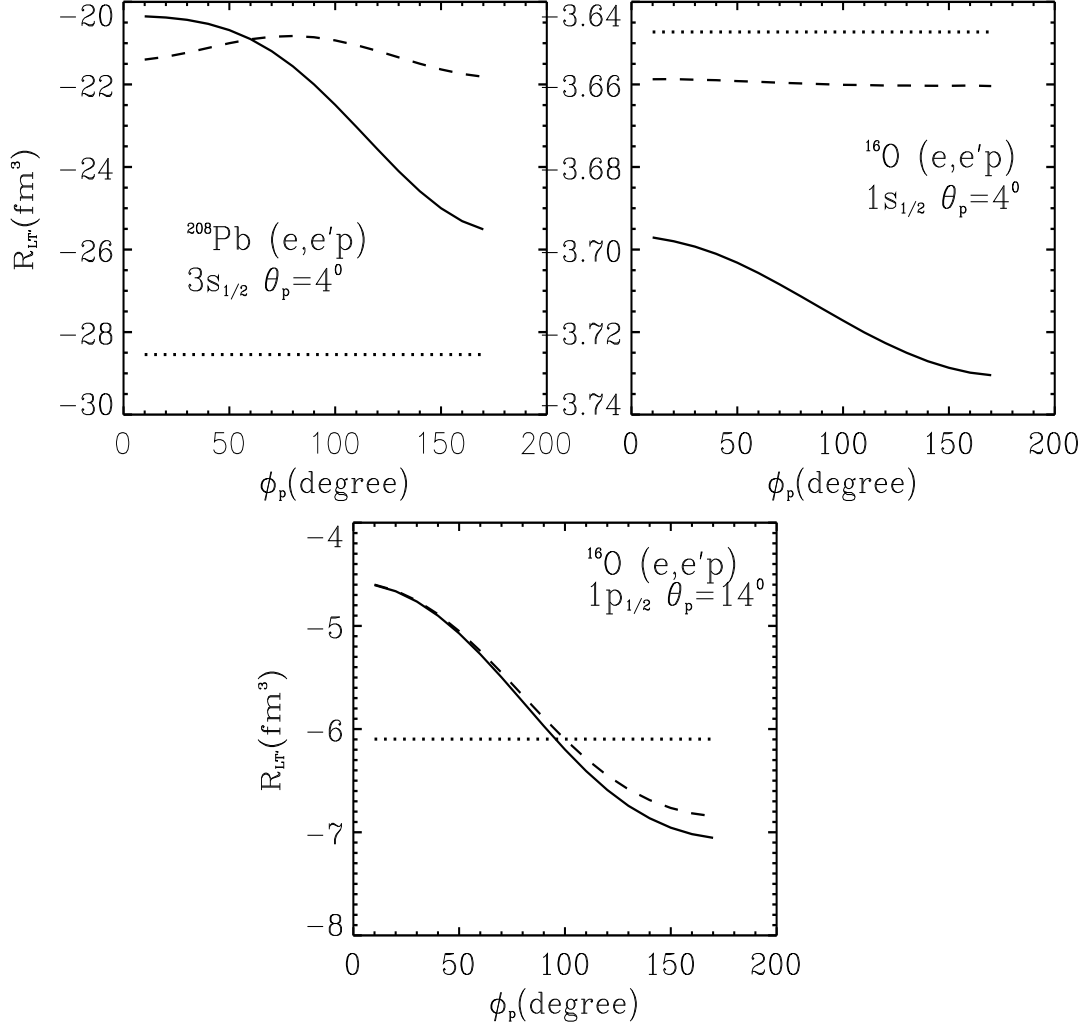


FIG. 11. The fifth structure function as a function of the azimuthal angle ϕ_P for $^{208}\text{Pb}(e, e'p)$ from the $3s_{1/2}$ shell and for $^{16}\text{O}(e, e'p)$ from the $1s_{1/2}$ shell and the $1p_{1/2}$ shell. The dotted line is the fifth structure function for PWBA, the solid line is the fifth structure function with $\hat{\mathbf{z}}$ axis along the asymptotic momentum \mathbf{q} , and the dashed line is for the case of the $\hat{\mathbf{z}}$ axis along the momentum transfer $\mathbf{q}'(R)$.

REFERENCES

- [1] Yanhe Jin, Ph.D, Dissertation, Ohio University (1991).
- [2] Yanhe Jin, D. S. Onley, and L. E. Wright, Phys. Rev. C **45**, 1311 (1992)
- [3] Yanhe Jin, D. S. Onley, and L. E. Wright, Phys. Rev. C **45**, 1333 (1992).
- [4] Yanhe Jin, D. S. Onley and L. E. Wright, Phys. Rev. C **50**, 168 (1994).
- [5] C. J. Horowitz, and B. D. Serot, Nucl. Phys. **A368**, 503 (1981).
- [6] Jian-Kang Zhang, Ph.D. Dissertation, Ohio University (1991).
- [7] S. Hama, B. C. Clark, E. D. Cooper, H. S. Sherif, and R. L. Mercer, Phys. Rev. C **41**, 2737 (1990).
- [8] K. S. Kim, L. E. Wright, Yanhe Jin, and D. W. Kosik Phys. Rev. C **54**, 2415 (1996).
- [9] K. S. Kim, Ph.D, Dissertation, Ohio University (1996).
- [10] F. Lenz and R. Rosenfelder, Nucl. Phys. **A176**, 513 (1971);
F. Lenz, thesis, Freiburg (1971).
- [11] J. Knoll, Nucl. Phys. **A201**, 462 (1974).
- [12] C. Giusti and F. D. Pacati, Nucl. Phys. **A473**, 717 (1987).
- [13] M. Trani, Phys. Lett. B **213**, 1 (1988);
M. Traini, S. Turck-Chieze, and A. Zghiche, Phys. Rev. C **38**, 2799 (1988).
- [14] T. DeForest Jr., Nucl. Phys. **A392**, 232 (1983).
- [15] L. Lapikás, Nucl. Phys. **A553**, 297 (1993).
- [16] G. J. Kramer, Ph.D. dissertation, University of Amsterdam (1990).
- [17] I. Bobeldijk, *et al.*, Phys. Rev. Lett. **73**, 2684 (1994).
- [18] V. Van der Sluys, J. Ryckebusch, and M. Waroquiur, Phys. Rev. C **54**, 1322 (1996).

- [19] J.M. Udias, P. Sarriguren, E. Moya de Guerra and J.A. Caballero, Phys. Rev. **C53**, R1488 (1996).